Analysis of the Impact of the Consolidated Material on the Morphology of Briquettes Produced in a Roller Press

Michał Bembenek (iD)*, Amelia Zięba, Mateusz Kopyściański, and Janusz Krawczyk1*

This article presents the results of saddle-shaped briquettes produced in a roller press from 15 fine-grained materials subjected to long-term seasoning. Experiments were carried out to determine the capacity of agglomerates, their surface roughness, compressive strength, excessive material, and superficial defects. Althoug`h a molding surface with molding cavities with the same shape was used for briquetting, significantly different results were obtained due to the different types of materials used for briquetting. Briquettes made from metallic and inorganic materials were characterized by a strength that increased with their density, which was not observed in carbonaceous materials. The tests are innovative and should be considered as pilot tests.

1. Introduction

The consolidation of dusty or fine-grained materials offers many benefits (Ref 1-6). A widely used method for the consolidation of loose materials involves pressurized agglomeration (Ref 7, 8). This process involves exerting pressure on a material that causes the grains to move closer and form many types of strong bonds (Ref 8). The product of the pressurized agglomeration process is compact shapes with relativity low porosity and specific mechanical strength, the sizes of which can be up to several thousand times larger than the input material grains (Ref 7-9). The continuity of the process ensures a smaller energy demand and a longer molding element and roll press lifetime compared with other industrial briquetting machines, e.g., screw or punch ones (Ref 10-16). Due to the diverse properties of fine-grained materials, the requirements set forth for blocks are met if the configuration and design properties of the roller press compaction system are correctly selected (Ref 17). Mutual differentiation of the working surfaces of both rolls prevents unfavorable phenomena from occurring during material consolidation (Ref 18, 19). In this way, an asymmetric compaction unit is established (Fig. 1). This is particularly useful for materials that are difficult to briquette in a roller press, i.e., those that are characterized by high moisture, high compaction degree necessary for consolidation, low bulk density, the presence of hydrophobic grains, those that tend to be suspended in hoppers and dispensers, and those with a high elastic deflection after pressure is removed. The use of an asymmetric compaction unit enables an increase in the moisture range within which the material can be briquetted (Ref 11, 20). It also eliminates briquettes from cracking in half along the plane of mutual closure of cavities on both rolls (Ref 18, 20). This results from a more favorable and uniform distribution of pressure exerted on the briquette being molded (Fig. 2) compared with the distribution obtained in a symmetrical system (Ref 20) and, consequently, a better material deformation distribution in the molding cavities (Fig. 3) (Ref 21). The essential factor observed over the many years that roller presses have been operated is that the briquetting of materials with various properties, despite using the same molding cavities, does not produce briquettes with the same shapes. Additionally, their volumes are usually smaller or bigger than the rated one, and, depending on the properties of the raw material, different defects appear on the agglomerate surfaces. Briquette materials may also have different storage properties; thus, the briquettes produced from different materials underwent morphological tests after long-term seasoning. The results provide technologically important information about the impact of the material type on the ability to make briquettes and their resulting durability, which limits the assessment of their flowability, compactness, and geometric features. This work analyzes the briquette from the perspective of materials engineering, due to there being an indication of the interactions between structure, properties, manufacturing technology, and the use of resulting briquettes. The analysis is based on the basic physical, chemical, and mechanical properties of the briquetted material.

Michał Bembenek, AGH University of Science and Technology, Faculty of Mechanical Engineering and Robotics, al. A. Mickiewicza 30, 30-059 Kraków, Poland; **Amelia Zięba**, Institute of Metallurgy and Materials Science of Polish Academy of Sciences, ul. Reymonta 25, 30-059 Kraków, Poland; **Mateusz Kopyściański** and **Janusz Krawczyk**, AGH University of Science and Technology, Faculty of Metals Engineering and Industrial Computer Science, al. A. Mickiewicza 30, 30-059 Kraków, Poland. Contact e-„mails: bembenek@agh.edu.pl, a.zieba@imim.pl, mkopys@agh.edu.pl, and jkrawcz@agh.edu.pl.

2. Materials and Methods

The first stage of the tests was to consolidate the materials to produce briquettes. This was done using a roller press with a 450-mm roll pitch diameter with an installed compaction unit for producing saddle-shaped briquettes (Fig. 1b) with a rated capacity of 6.5 cm³. The outline view of the molding surface used to consolidate the material is presented in Fig. 4. The press was equipped with a cycloidal gear motor with a power of 22 kW and a frequency converter that enabled infinitely variable control of the revolutionary speed of the rolls. All materials were consolidated using a gravity feeder with a roller revolutionary speed of 4.25 rpm, which corresponded to the peripheral speed of the rolls equal to 0.1 m/s with an inter-roll gap of 1 mm. After production, the briquettes were seasoned at room temperature for 10 ± 2 years. Fifteen materials were used for tests, which were classified into three groups: materials of organic origin, metallurgical and heavy industry waste, and materials of inorganic origin. Before the consolidation process, the materials were thoroughly mixed and brought to a proper moisture h (provided with the material) enabling them to be consolidated in a roller press. A binder was added to some of them.

The following raw materials were included in the carbonic materials:

- lignite (Poland) ($h=21\%$)—marked with the symbol A,
- coal dust with 1% carboxymethyl cellulose ($h=25\%$)—marked with the symbol B,
- graphite dust with residual limestone dust (2.5%), and molasses (8%) ($h=5.2\%$)—marked with the symbol C.

The following raw materials have been classified as metallurgical and heavy industry waste:

- manganese dust with water glass (8%) ($h=3.5\%$)—marked with the symbol D,
- mill scale with calcium hydroxide (5%) and molasses (5%) ($h=2.0\%$)—marked with the symbol E,
- BOF sludge with calcium oxide (13%), fine coke (13%) and molasses (8%) ($h=10.5\%$)—marked with the symbol F,
- manganese blast furnace dust with waste from a metallurgical felling machine (8.5%) and molasses (10%) ($h=$ 4.0%)—marked with the symbol G,
- ferrosilicon with water glass (8%) ($h=3.0\%$)—marked with the symbol H,
- waste blasting sludge with molasses (8%), ($h=12.8\%$)—marked with the symbol I,
- scale with molasses (6%) ($h=2.5\%$)—marked with the symbol J,
- shavings from bearing alloys—marked with the symbol K,
- zinc oxide with sulfite (8%) ($h=3.0\%$)—marked with the symbol L.

The materials of inorganic origin were:

- phosphorite ($h=3.0\%$)—marked with the symbol M,
- sodium tripolyphosphate—marked with the symbol N,
- calcium fluoride ($h=14.5\%$)—marked with the symbol O.

To compare the volume of the tested briquettes with the rated value, we measured the projection of the largest area of the samples and the maximum thickness along the direction normal to the projection. Based on this information and the known volume of the model briquette formed from a completely filled forming cavity, the real volume of briquettes was determined according to the formula:

$$V_{rz} = V_{rz_b} \cdot \frac{V_{teoret}}{V_{teoret_b}} \left(mm^3\right)$$

where V_{rz_b}—volume capacity of a cuboid designed based on the projection area and the largest thickness of the tested briquette (mm³), V_{teoret}—theoretical briquette volume capacity
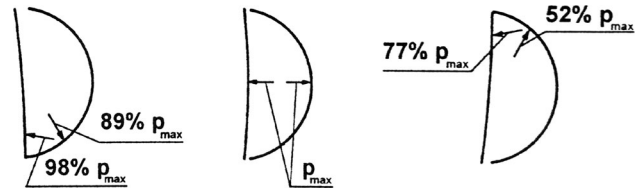

Fig. 2 Scheme illustrating the quantitative nature of unit pressure changes during the briquetting process in a roll press with an asymmetric compaction unit, p_{max}—maximum unit pressure (Ref 19)
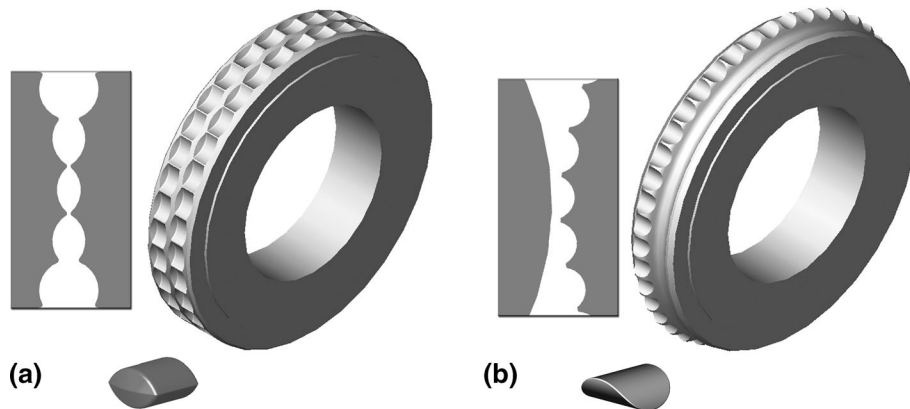

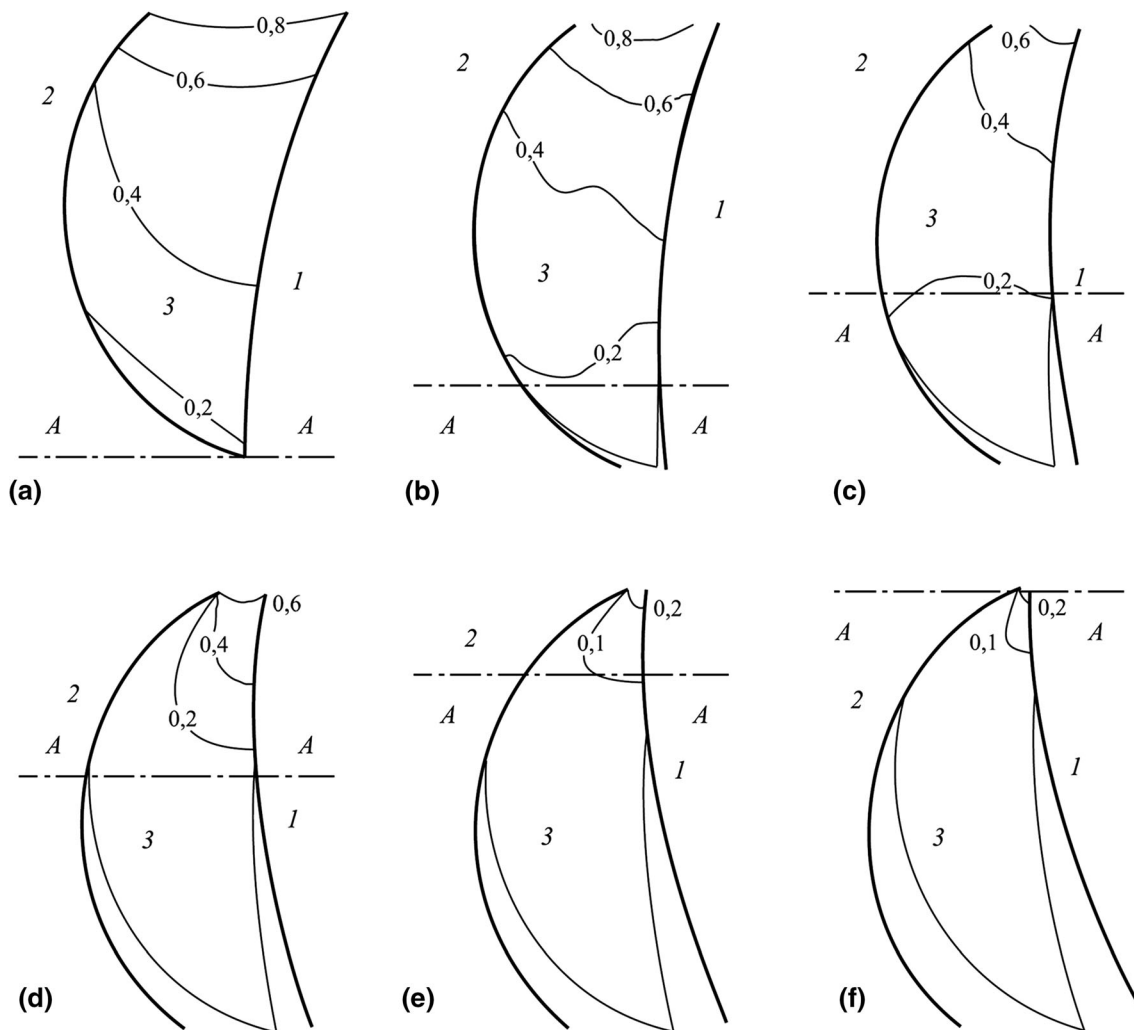**Fig. 1** Molding rings used in roll press compaction systems: (a) symmetric, (b) asymmetric

Fig. 3 Deformation distribution during briquetting in roll press with an asymmetric unit: 1—smooth roll, 2—radial profile, 3—briquette, a, b, c, d, e, f—sequence of roll rotation in increments of 5°, A–A—position of the line connecting the centers of the rolls (Ref 20)
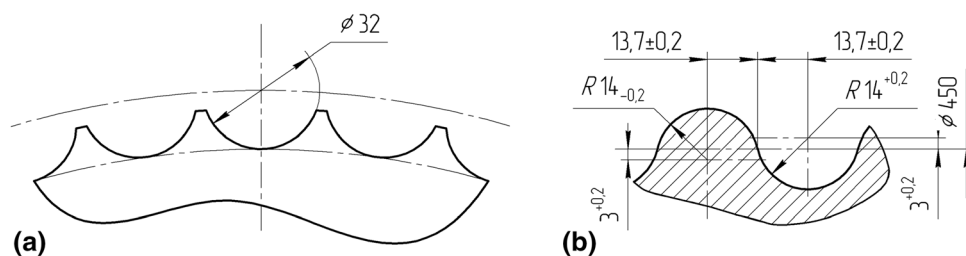

Fig. 4 Geometry of molding cavities on the working surface of rolls used for tests: (a) front view, (b) cross section through the groove

due to the die geometry (mm^3), and V_{teoret_b}—volume of a cuboid determined based on the projection area and the largest thickness for the benchmark briquette model (mm^3).

The surface area was determined based on an image of the briquettes using LabVIEW environment with Vision Assistant. Also, the area of material allowances and losses was measured against the rated outline of the molding die element that was theoretically determined from a briquette model developed

using CAD software. Due to the dimensional and geometric diversity, each briquette was rescaled to make its outline without allowances overlap with the theoretical outline. A measurement performed for four briquettes for each of the tested materials was considered to be representative. To determine the density of the briquettes, their weight was measured using a SA-120CE laboratory scale by Shinko Denshi. To examine the surface structure properties, roughness

measurements were performed and macrophotographs of the briquette surfaces were taken. The roughness measurements were performed using a Veeco WykoNT9300 optical profilometer. Measurements were performed in the central part of the surface of each tested briquette. The R_a parameter was determined—the average arithmetical deviation of the roughness profile from the average line. Surface structure observations were performed in the central part of the briquette using an Axiovert 200 MAT optical microscope by Carl Zeiss. To compare the diversified morphology of the briquette surfaces, four features of the surface were introduced, and their share in each material was determined. To compare the strength of the briquettes, hardness measurements were carried out based on the Leeb dynamic method. An Equotip Bambino 2 hardness meter with a type D universal head was used, and the test was repeated four times for each of the tested materials in the central part of the briquette surface. Based on the surface hardness of the briquettes, their compressive strengths were estimated using the relationship (Ref 22):

$$\sigma_c = 3,1335 \cdot e^{0,0051 \cdot HLD} (MPa) \qquad (Eq\ 1)$$

where σ_c—compressive strength (MPa) and HLD—Leeb hardness (HLD).

3. Results and Discussion

Figure 5 presents images of all briquettes made for tests. The measured thickness range of the briquettes for each material and the range of areas of allowances and losses compared with an ideal rendering of the die shape are presented in Figs. 6 and 7. It varied and was strongly dependent on the properties of the consolidated material. For most materials, the thickness of the briquette was greater than the theoretical value obtained from the die geometry. This was observed in all samples from the group of briquettes made from metallurgical and heavy industry waste, except zinc oxide with a binder and inorganic materials. This discrepancy resulted from the fact that the materials were consolidated in roller presses partly within the elastic strain range and expanded when the pressure was released. This is referred to in the literature as *relaxation* (Ref 11). This relaxation increased the briquette dimensions compared with the rated dimensions of the molding die. For most briquettes made of carbonaceous materials, the briquette thickness was smaller or similar to the theoretical value. This may result from briquette delamination during consolidation, or from sample shrinkage due to a significant decrease in their moisture during seasoning. The briquettes also differed in their projection areas. Comparing their outline to the outline of the molding pocket shows allowances (the briquetted material protruded beyond
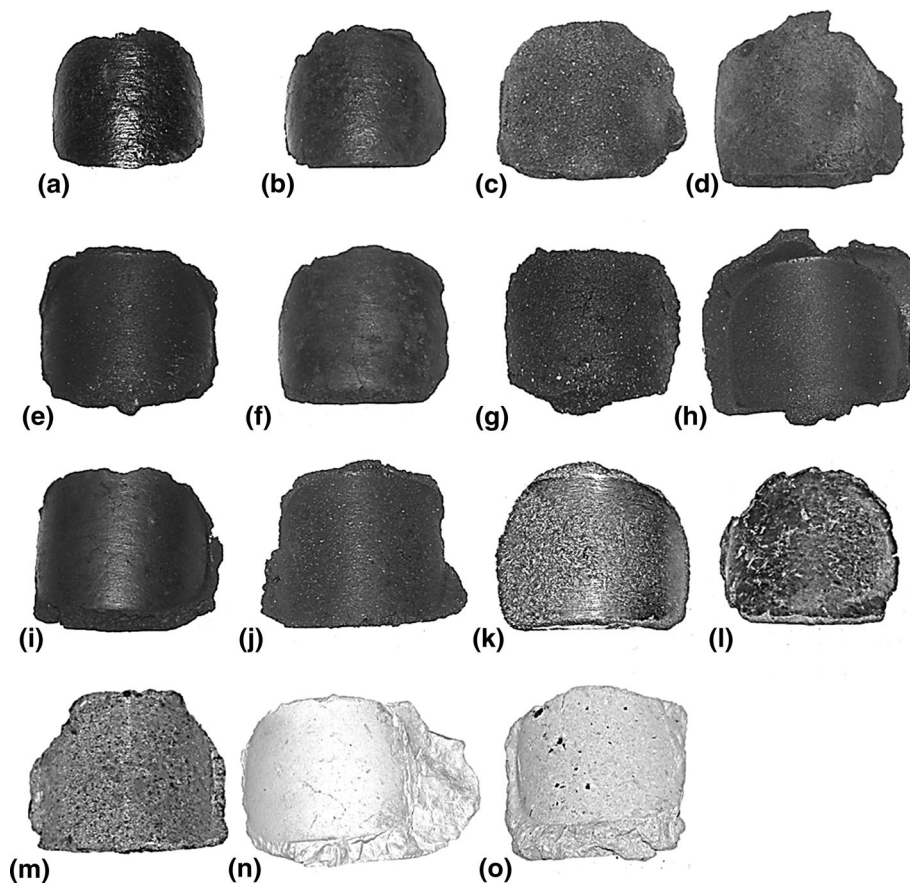

Fig. 5 View of tested briquettes: A—lignite (Poland), B—coal dust with binder, C—graphite dusts with binder, D—manganese dust with binder, E—mill scale with binder, F—BOF sludge with binder, G—manganese blast furnace dust with binder, H—ferrosilicon with binder, I—waste blasting sludge with binder, J—scale with binder, K—shavings from bearing alloys without binder, L—zinc oxide with binder, M—phosphorite, N—sodium tripolyphosphate, O—calcium fluoride without binder
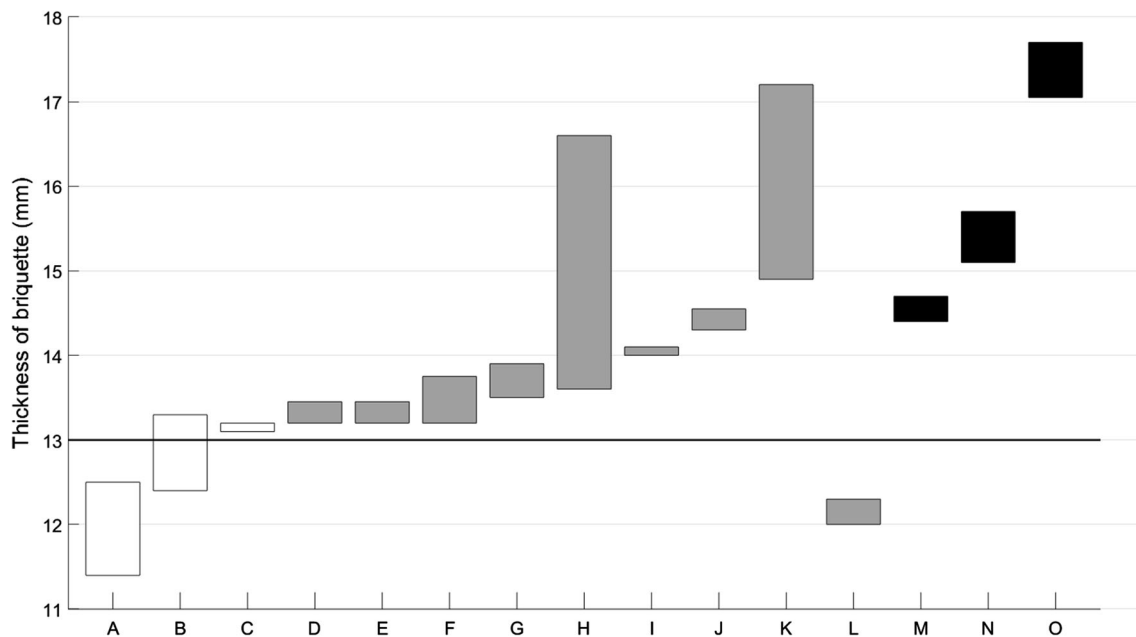
Fig. 6 Thickness of tested briquettes with reference to the theoretical value (13 mm): A—lignite (Poland), B—coal dust with binder, C—graphite dusts with binder, D—manganese dust with binder, E—mill scale with binder, F—BOF sludge with binder, G—manganese blast furnace dust with binder, H—ferrosilicon with binder, I—waste blasting sludge with binder, J—scale with binder, K—shavings from bearing alloys without binder, L—zinc oxide with binder, M—phosphorite, N—sodium tripolyphosphate, O—calcium fluoride without binder

the seat) and losses (the material within the edges crumbled off). The briquettes made of lignite and coal dust with binder showed the largest loss areas, which indicated fragile cracking of the material at the briquette edges and crumbling off in other parts of the material. Most briquettes (except zinc oxide with binder) showed significant allowance areas, demonstrating the plastic properties of the consolidated materials, which was related to the inaccuracy of the molding method.

The surface structure test results of the examined briquettes differed depending on the type of briquettes material, but they did not differ within the material groups. Four main surface morphology features were observed: cracking, scratches, crumbling, and granularity. The presence of cracking and crumbling (Fig. 8a and c) indicated a fragile cracking of the surface layer due to tension acting on the material during consolidation in a molding die. Such features were observed on the surface structure of samples of waste blasting sludge with binder and lignite. Scratches formed (Fig. 8b) due to relative motion at the briquetted material–molding interface which caused grooving and micro-cutting on the newly formed surface. This can be seen on the surface image of briquettes with zinc oxide/binder. Such interactions between the consolidated materials and the die also contributed to the rapid destruction of the molding cavity elements (Ref 23). The granularity (Fig. 8d) may indicate small plastic deformation of the material being consolidated and fragile properties of particles being consolidated, which made it difficult for material bridges to form. This feature was observed in the materials, which causes difficulties during molding. The granularity may also be a result of the

crumbling of the surface layer of the briquette during formation —the highly granular surface was a fracture surface formed after the material cracked and crumbled off, as visible on the surface of mill scale and binder samples. Among the briquettes made of inorganic materials, some did not have clearly distinguished surface properties (sodium tripolyphosphate, calcium fluoride). Such homogeneous surfaces showed that the structure of the briquettes being molded was not damaged nor was there a distinctive friction interaction between the die part and the surface during consolidation. This was the best outcome due to the properties of the briquette and the lower consumption of the molding surface and clear symptoms of tribological wear (Ref 24).

The granularity share on the surface of the briquettes is related to the R_a roughness parameter in all examined briquette groups. Higher R_a values were not observed at higher granularity. Other surface morphology features were not directly reflected by R_a.

Figure 9 presents a summary of the relationships between the compressive strength of the tested briquettes and their density.

The briquettes of carbonic origin and metallurgical and heavy industry waste origin showed the highest specific strength among the tested groups, while the briquettes made of materials of metallic origin showed the lowest. The strength increased with the density for the briquettes made from metallurgical and heavy industry waste and inorganic materials. The opposite trend was observed for briquettes made of
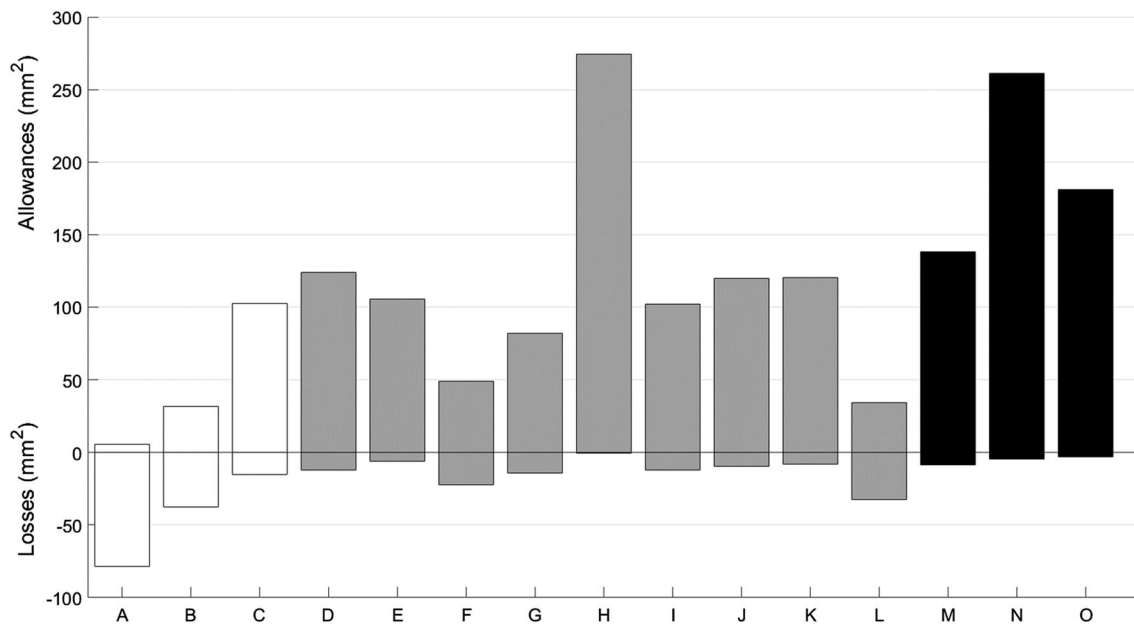
Fig. 7 Projection geometry inaccuracies of the tested briquettes—areas of allowances (referred to as positive values) and losses (referred to as negative values) relative to an ideal shape: A—lignite (Poland), B—coal dust with binder, C—graphite dusts with binder, D—manganese dust with binder, E—mill scale with binder, F—BOF sludge with binder, G—manganese blast furnace dust with binder, H—ferrosilicon with binder, I—waste blasting sludge with binder, J—scale with binder, K—shavings from bearing alloys without binder, L—zinc oxide with binder, M—phosphorite, N—sodium tripolyphosphate, O—calcium fluoride without binder
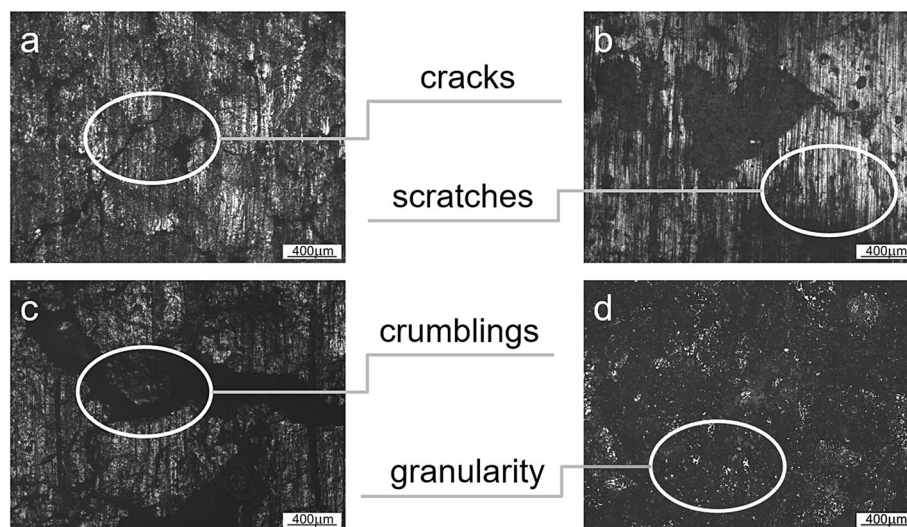

Fig. 8 Observed main features of the briquette surface morphology: (a) cracks—waste blasting sludge with binder, (b) scratches—zinc oxide with binder, (c) crumbling—lignite, (d) granularity—mill scale with binder

carbonaceous materials—the increased density followed a deterioration in the strength properties.

Based on the summary of the compressive strength and R_a (Fig. 10), it can be stated that the surface roughness of the produced briquettes increased with the strength. This was related to the fact that the particles of briquettes with a higher strength were less susceptible to plastic deformation. In some briquettes, the friction at the interface of the material being consolidated and the molding tool produced numerous grooves and scratches. This initiated surface cracking and increased the
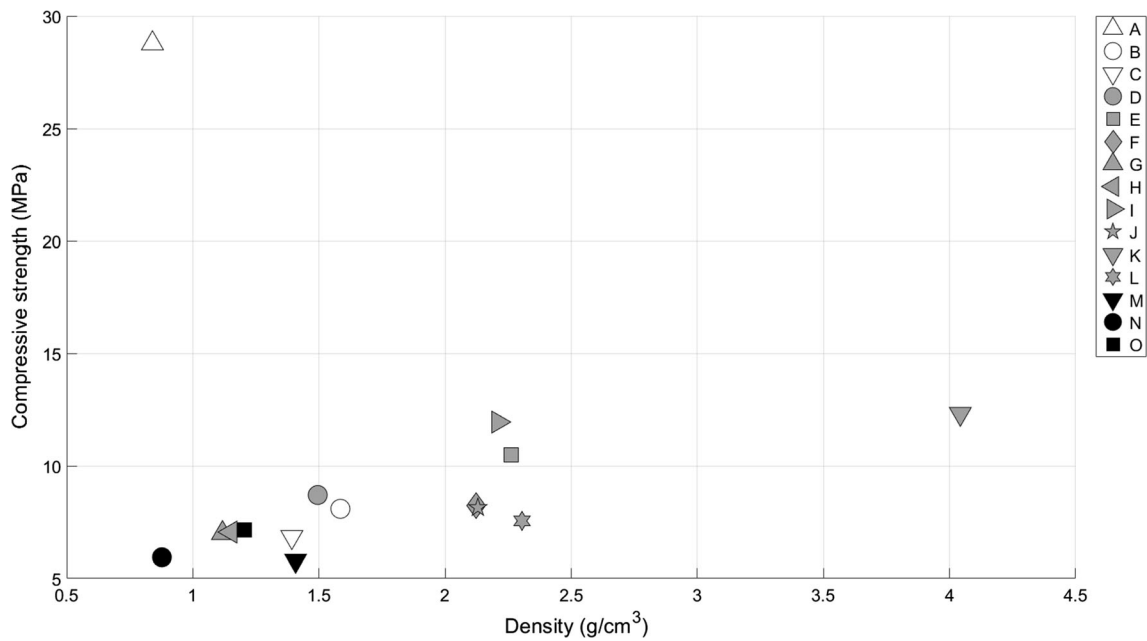
Fig. 9 Compressive strength juxtaposed with the briquette densities: A—lignite (Poland), B—coal dust with binder, C—graphite dusts with binder, D—manganese dust with binder, E—mill scale with binder, F—BOF sludge with binder, G—manganese blast furnace dust with binder, H—ferrosilicon with binder, I—waste blasting sludge with binder, J—scale with binder, K—shavings from bearing alloys without binder, L—zinc oxide with binder, M—phosphorite, N—sodium tripolyphosphate, O—calcium fluoride without binder
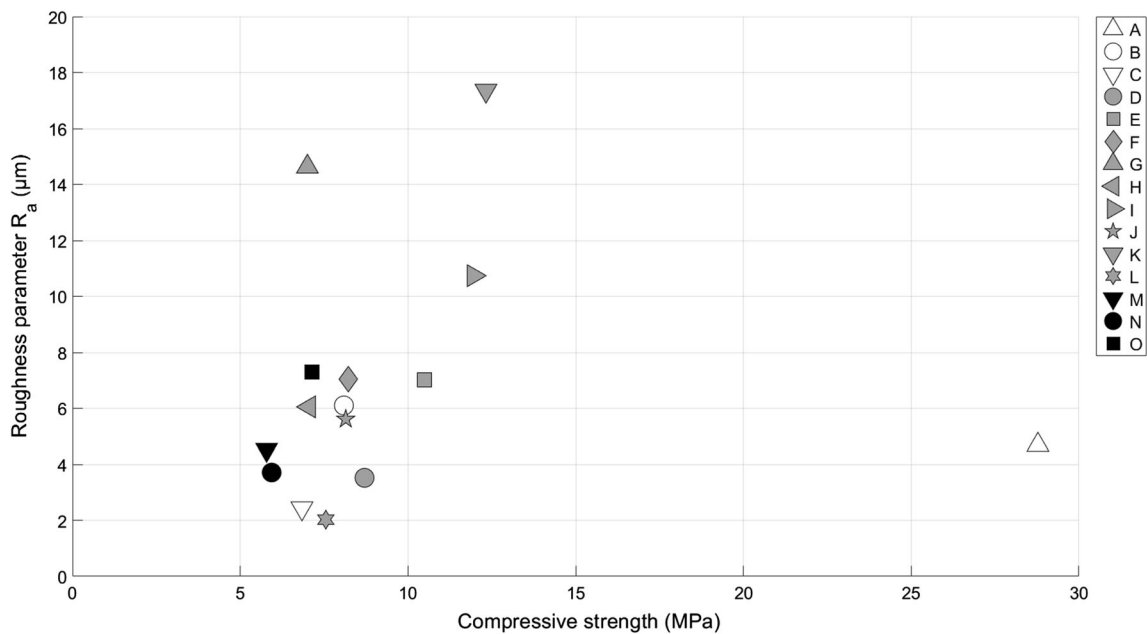

Fig. 10 The R_a roughness parameters juxtaposed with the compressive strength of briquettes: A—lignite (Poland), B—coal dust with binder, C—graphite dusts with binder, D—manganese dust with binder, E—mill scale with binder, F—BOF sludge with binder, G—manganese blast furnace dust with binder, H—ferrosilicon with binder, I—waste blasting sludge with binder, J—scale with binder, K—shavings from bearing alloys without binder, L—zinc oxide with binder, M—phosphorite, N—sodium tripolyphosphate, O—calcium fluoride without binder

roughness. This was best demonstrated in the briquettes made of waste blasting sludge with binder and manganese blast furnace dust with a binder. The high roughness of the shavings from bearing alloys without binder arose due to the structure of the chips preserved on the briquette surface.

4. Conclusion

The compaction method employed for all tested materials did not cause briquettes to break in half along the plane of

mutual closure of cavities on both rolls. Shrinkage occurred mainly in briquettes containing carbonaceous materials following the briquetting process. In nearly all materials, an increase in the compressive strength of the briquettes also increased the surface roughness R_a. It was also found that the strength of the briquettes made of metallic and inorganic materials increases with their density, which was not observed in carbonaceous materials. The microscopic surface examinations made it possible to distinguish four major features of the surface morphology of the briquettes, i.e., cracking, scratches, crumbling, and granularity.

Open Access

References

1. A. Kraszkiewicz, M. Kachel-Jakubowska, and E. Lorencowicz, Influence of Cellulose Content in Plant Biomass on Selected Qualitative Traits of Pellets, *Agric. Agric. Sci. Procedia*, 2015, **7**, p 125–130. https://doi.org/10.1016/j.aaspro.2015.12.005
2. H.A. Ajimotokan, A.O. Ehindero, K.S. Ajao, A.A. Adeleke, P.P. Ikubanni, and Y.L. Shuaib-Babata, Combustion Characteristics of Fuel Briquettes Made from Charcoal Particles and Sawdust Agglomerates, *Sci. Afr.*, 2019, https://doi.org/10.1016/j.sciaf.2019.e00202
3. D. Andrejko and J. Grochowicz, Effect of the Moisture Content on Compression Energy and Strength Characteristic of Lupine Briquettes, *J. Food Eng.*, 2007, **83**, p 116–120
4. M.J. Blesa, V. Fierro, J.L. Miranda, R. Moliner, and J.M. Palacios, Effect of the Pyrolysis Process on the Physicochemical and Mechanical Properties of Smokeless Fuel Briquettes, *Fuel Process. Technol.*, 2001, **74**, p 1–17
5. L. Florentino-Madiedo, E. Díaz-Faes, and C. Barriocanal, Mechanical Strength of Bio-coke from Briquettes, *Renew. Energy*, 2020, **146**, p 1717–1724
6. S. Galen and A. Zavaliangos, Strength Anisotropy in Cold Compacted Ductile and Brittle Powders, *Acta Mater.*, 2005, **53**, p 4801–4815
7. E.F. Aransiola, T.F. Oyewusi, J.A. Osunbitan, and L.A.O. Ogunjimi, Effect of Binder Type, Binder Concentration and Compacting Pressure on Some Physical Properties of Carbonized Corncob Briquette, *Energy Rep.*, 2019, **5**, p 909–918. https://doi.org/10.1016/j.egyr.2019.07.011
8. W. Pietsch, An Interdisciplinary Approach to Size Enlargement by Agglomeration, *Powder Technol.*, 2003, **130**, p 8–13
9. A. Michrafy, A. Zavaliangos, and J.C. Cunningham, Dry Granulation Process Modeling, *Predict. Model. Pharm. Unit Oper.*, 2017, **1**, p 71–97. https://doi.org/10.1016/B978-0-08-100154-7.00004-1
10. G. Bindhumadhavan, J.P.K. Seville, M.J. Adams, R.W. Greenwood, and S. Fitzpatrick, Roll Compaction of a Pharmaceutical Excipient: Experimental Validation of Rolling Theory for Granular Solids, *Chem. Eng. Sci.*, 2005, **60**, p 3891–3897
11. M. Bembenek, Research and Prospects for New Areas of Using Roller Presses (Badania i perspektywy nowych obszarów stosowania pras walcowych), *Przem. Chem.*, 2017, **9**(96), p 1845–1847. https://doi.org/10.15199/62.2017.9.3 (in Polish)
12. S. Obidziński, Pelletization Process of Postproduction Plant Waste, *Int. Agrophisics*, 2012, **3**(26), p 279–284
13. P. Guigon and O. Simon, Roll Press Design—Influence of Force Feed Systems on Compaction, *Powder Technol.*, 2003, **130**, p 41–48
14. A. Khudyakov, S.V. Vashchenko, K.V. Baiul, and Y.S. Semenov, Kaolin Raw Material Briquetting for Lump Chamotte Production, *Refract. Ind. Ceram*, 2018, **4**(58), p 333–337. https://doi.org/10.1007/s11148-018-0231-3
15. K.V. Baiul, Synthesis of Roller Press Rational Design for Composite Solid Fuel Production, *Probl. Reg. Energ.*, 2019, **2**(43), p 103–116. https://doi.org/10.5281/zenodo.3367048
16. A. Mroziński, J. Flizikowski, A. Tomporowski, W. Kruszelnicka, I. Piasecka, R. Kasner, Robert, Research of Wood Biomass Briquetting Process, 2018. https://doi.org/10.13140/rg.2.2.14931.89128
17. Z. Drzymała, *Industrial Briquetting—Fundamentals and Methods*, Elsevier, Warsaw, 1993
18. A. Janewicz, B. Kosturkiewicz, and M. Hryniewicz, Comparative Tests of the Briquetting Process in New Asymmetrical Compacting Systems of Roller Presses (Badania porównawcze brykietowania w nowych asymetrycznych układach zagęszczania pras walcowych), *Przem. Chem.*, 2018, **8**(97), p 1363–1366. https://doi.org/10.15199/62.2018.8.25 (in Polish)
19. V.I. Polyanskii, M.V. Kobelev, and A.V. Vetoshkin, The Equipment for the Press Compacting of the Metallurgical Lime Screenings (Оборудование для брикетирования отсева металлургической извести), *N. Refract. Sci. Eng. J.*, 2014, **3**, p 99–100 (in Russian)
20. M. Hryniewicz, *Method of Selection of Roll Presses and Elaboration of Design Criteria for Their Modernization or Construction (Metoda doboru pras walcowych oraz opracowania założeń do ich modernizacji lub konstrukcji)*, AGH University of Science and Technology, Kraków, 1997 (in Polish)
21. Y.N. Loginov, N.A. Babaylov, and D.N. Pervukhina, Physical Modeling of Roll Pressing at Asymmetric Effect on the Sealing Material (Физическое моделирование валкового прессования при несимметричном воздействии на уплотняемый материал), *News High. Educ. Inst. Ferrous Metall. (Известия Высших Учебных Заведений. Черная Металлургия)*, 2015, **3**(58), p 186–191 (in Russian)
22. Y. Asiri, *Standardized Process for Filed Estimation of Unconfined Compressive Strength Using Leeb Hardness*, Dalhousie University, Halifax, 2017
23. M. Bembenek, *Innovations in the Design and Use of Roller Presses (Innowacje w konstrukcji i zastosowaniu pras walcowych)*, AGH University of Science and Technology, Kraków, 2018 (in Polish)
24. M. Hryniewicz, Investigation into Increase of the Durability of Briquetters Forming Elements (Badania nad zwiększeniem trwałości elementów formujących brykieciarek), Scientific Magazine of the Bialystok University of Technology, *Tech. Stud. Constr. Oper. Mach.*, 2001, **8**(139), p 135–142 (in Polish)